Substituent Effects in the Migration Step of the Baeyer−Villiger Rearrangement. A Theoretical Study

Lino Reyes,*,† Miguel Castro,‡ Julián Cruz,‡ and Manuel Rubio§

Depto. de Química Orgánica and Depto. de Física y Química Teórica, DEPg, Facultad de Química, Universidad Nacional Autónoma de México, Del. Coyoacán, México, D. F., C.P. 04510, México, and Instituto de Química Universidad Nacional Autónoma de México, Del. Coyoacán, México, D.F., C.P. 04510, México

Received: July 27, 2004; In Final Form: February 17, 2005

Quantum mechanical calculations have been performed on the migration step of the Baeyer−Villiger (BV) rearrangements of some acetophenones, *p*-$RC_6H_4COCH_3$ (R = CN, Cl, H, CH_3, CH_3O) with *m*-chloroperbenzoic acid. The energy barriers, charge distributions, and frontier molecular orbitals determined for the aryl migration step explain the effects of substituents on the reactivity of these ketones. A plot of the log of relative oxidation rates of the ketones versus their corresponding calculated energy barriers of the migration stage showed a downward deviation for the *p*-OCH_3 derivative. This result is consistent with a change in the rate-determining step, from the aryl migration to the carbonyl addition, in the case of *p*-methoxyacetophenone, according to the suggestion that the rate-determining step of the BV oxidation can change with variations in the substituent group.

1. Introduction

The Baeyer−Villiger (BV) reaction, a process by which ketones are converted into esters or lactones,[1] is of great significance in organic synthesis. As a result, it has been extensively studied experimentally for about 100 years, and it is the subject of many publications.[2−4] It is well-known that the reaction occurs in a two-stage mechanism. In the first step, the carbonyl addition of a peroxyacid to ketones or aldehydes produces a tetrahedral adduct called the Criegee intermediate.[5] The second step is the migration of the alkyl or aryl group from the ketone moiety to one of the two peroxide oxygens of the peracid part in the intermediate. The latter is accepted to be the rate-determining step, involving a concerted mechanism; namely, the migration is simultaneous with the departure of the acid group.[6] However, some kinetic results for the reaction have demonstrated ambiguity in the rate-determining step.[7−12] It has been observed that, when the ketone is not symmetric, the steric and electronic factors significantly affect the migratory ability,[2] though other factors may also be involved.[11,12] In general, the ketonic substituent with better ability to stabilize a carbocation will rearrange preferentially;[3] however, this assumption hardly explains the regioselectivity of the BV reaction of bicyclic systems.[35,36] It is well-accepted that the migrating group alignment needs to be anti-periplanar to the O−O bond of the leaving peroxyacid;[18] this orientation allows the σ orbital of the migrating substituent to overlap with the σ^* orbital of the peroxide bond. This requirement has been referred to as the primary stereoelectronic effect, and it was invoked by Crudden[40] to explain the migratory preference of electron-deficient CHF over the unsubstituted methylene in the BV oxidation of *cis*-4-*tert*-butyl-2-fluorocyclohexanone. Contrarily, normal regioselectivity was found in the BV oxidation of 2-trifluoromethylcyclohexanone.[14]

Although the effects of miscellaneous substituents on the rates of the BV rearrangement have long been investigated experimentally, little is known in detail about the relationship between the substitution pattern of the substrates and their reactivities. This has been explained by considering that in the BV oxidation several steps can be rate-determining depending on the substrate itself, peracid, and the reaction conditions.[3,15−17]

In the case of acetophenones, electron-donating substituents on the migrating phenyl group facilitate the BV rearrangement.[2] Many kinetic studies have been reported for the substituent effect of the BV reaction of these ketones. However, the results are still unclear regarding which step is the rate-determining step.[10−12] For instance, the migration in the BV reaction of para-substituted acetophenones, with *m*-chloroperbenzoic acid (*m*-CPBA) in chloroform, has been considered to be a rate-determining and concerted step by Palmer and Fry on the grounds of the negative ρ value for the Hammett plot and by the ^{14}C isotope effect observed.[10] Nevertheless, no isotope effect was detected for the exceptional case of *p*-methoxyacetophenone. This fact was explained by considering the strong electron-donating ability of the *p*-methoxy group. In contrast, Ogata and Sawaki proposed another explanation suggesting that the lack of isotope effect and a downward deviation, observed in the Hammett correlation for *p*-methoxyacetophenone, are consistent with a change of the rate-determining step from the migration to the carbonyl addition.[11]

Despite the importance of the BV reaction as a powerful method in organic synthesis and the relevant role that the substituent effects plays in the BV rearrangement, relatively few theoretical studies of its mechanism have been reported in the literature.[13,15,18−26] Some calculations have addressed the substituent effects on the BV oxidation.[15,21,23,24] The effects of the

* Corresponding author. Phone: +5255-56223802. Fax: +5255-56223806. E-mail: linoj@correo.unam.mx.

† Depto. de Química Orgánica, Universidad Nacional Autónoma de México,.

‡ Depto. de Física y Química Teórica, Universidad Nacional Autónoma de México.

§ Instituto de Química Universidad Nacional Autónoma de México.

10.1021/jp040512q CCC: $30.25
Published on Web 03/24/2005

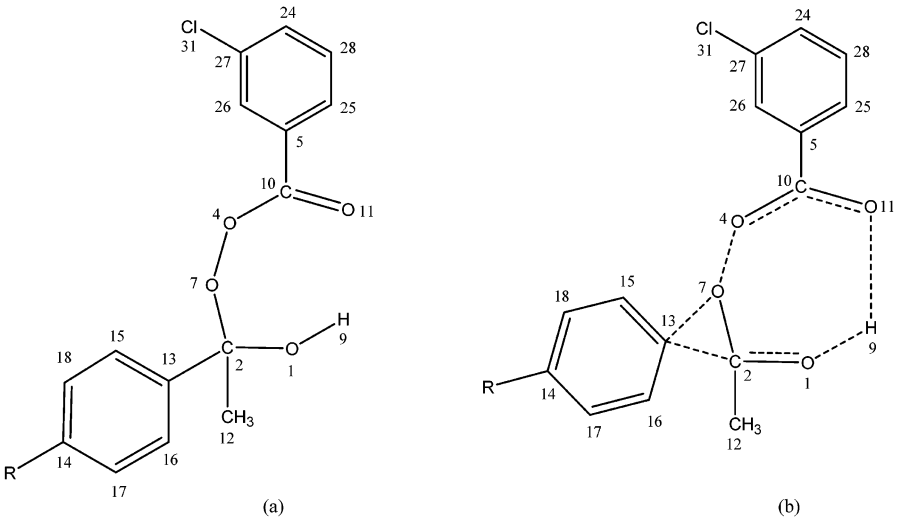

Figure 1. (a) Criegee intermediate. (b) Transition structure for the BV rearrangement. Broken lines represent bond-making/breaking in the TS.

p-OCH_3 group on the BV oxidation of *p*-methoxyacetophenone have been analyzed by Okuno,[15] in connection with an ab initio study of the noncatalyzed and catalyzed mechanisms for the BV reaction of benzaldehyde and *p*-anisaldehyde. He evaluated the free-energy change for these systems and showed that the mechanism of the BV oxidation can change with catalysis or substituent effects. This is in agreement with the explanation proposed by Ogata and Sawaki, in which the *p*-OCH_3 group induces a change of the BV mechanism, as quoted already.[11]

In our first study of this reaction using a simple model (performic acid and acetone),[22] we showed that the transition-state (TS) geometry associated with the BV rearrangement and the general orientation of the transition vectors are nearly invariant of the calculation method. More recently,[23] we used this finding to analyze the migration step on the BV reaction of acetone with some alkyl and aryl peracids by using AM1 and PM3 methods. To the best of our knowledge, there has not been a computational systematic study of the effect of both donor and acceptor substituents at every position of the migrating aryl group on the rates of the substrates in the BV reaction. In the present work, a theoretical study was performed to investigate the substituent effects on the rates of the BV rearrangement of para-substituted acetophenones. In particular, we calculated the Criegee intermediate (Figure 1a) and the TS (Figure 1b) for the migration step of the *m*-CPBA reaction with acetophenone, *p*-methylacetophenone, *p*-methoxyacetophenone, *p*-chloroacetophenone, and *p*-cyanoacetophenone. This study reproduces the main experimental patterns and provides insights into the origins of the substituent effects to elucidate their influence on this rearrangement. In fact, we have found important relations among the reactivity of these ketones with the energy barriers, charge distributions, frontier molecular orbitals, and bond orders obtained for the aryl migration step. Furthermore, our results provide evidence to support Okuno's suggestion that there is a change of the rate-determining step, from the migration to the carbonyl addition, in the case of *p*-methoxyacetophenone.

2. Computational Procedure

Calculations were carried out using the *Gaussian 98* program.[27] The geometries of the Criegee intermediate, the aryl group migration transition state, and the products were located with PM3 in *SPARTAN 02*[28] and fully optimized with HF/6-31G**. We have also optimized the HF/6-31G** structures for the parent system using the B3LYP functional with the 6-31G** and 6-31+G** basis sets. The obtained geometries and barriers, with both basis sets, are very similar to each other (Figure 2 and Table 1S in Supporting Information), so that in the present study B3LYP/6-31G** was selected to reduce computational time. A vibrational analysis was carried out for each optimized stationary point, indicating the nature of the structure: a minimum or a transition state. The energy barriers for aryl migration (relative to Criegee intermediate), ΔE, were estimated using B3LYP/6-31G** total electronic energies with zero-point vibrational energy (ZPE) corrections (Table 1S). The B3LYP functional has been shown to perform well for the prediction of structures and relative energies in processes involving O−O cleavage.[29] However, several studies indicate that B3LYP systematically underestimates barrier heights.[29−32] To compare, we have therefore also calculated MP2/6-31G**//B3LYP/6-31G** total energies. The charge distribution was evaluated by the natural population analysis[33] (NPA). Frontier molecular orbitals were also generated from the optimized geometries. The Mayer formulation was applied to obtain the bond order,[34] which was used to analyze the degree of synchronicity among the aryl migration and other bond breaking/making processes.

3. Results and Discussion

We have analyzed the influence of electron-donor groups (CH_3O, CH_3) and electron-withdrawing groups (CN, Cl) on the transition states, geometries, and energies of BV rearrangements, when substituted at the para position of the migrating aryl group. The following systems have been studied

$$ArCOCH_3 + m\text{-}ClC_6H_4CO_3H \rightarrow CH_3COOAr + m\text{-}ClC_6H_4CO_2H$$

where Ar = *p*-RC_6H_4 and R = CN, Cl, H, CH_3, CH_3O.

3.1. Geometries and Energies. Because our main interest in this study lies in the substituent effects on the transition states and the energy barriers in the rearrangements, this paper focuses on the results that are related to the TS of this stage. Also, the optimized geometries for reactants and products were obtained at the HF/6-31G** and B3LYP/6-31G** levels of theory. In general, the HF/6-31G** optimizations reproduce well the trends of the B3LYP/6-31G** results.

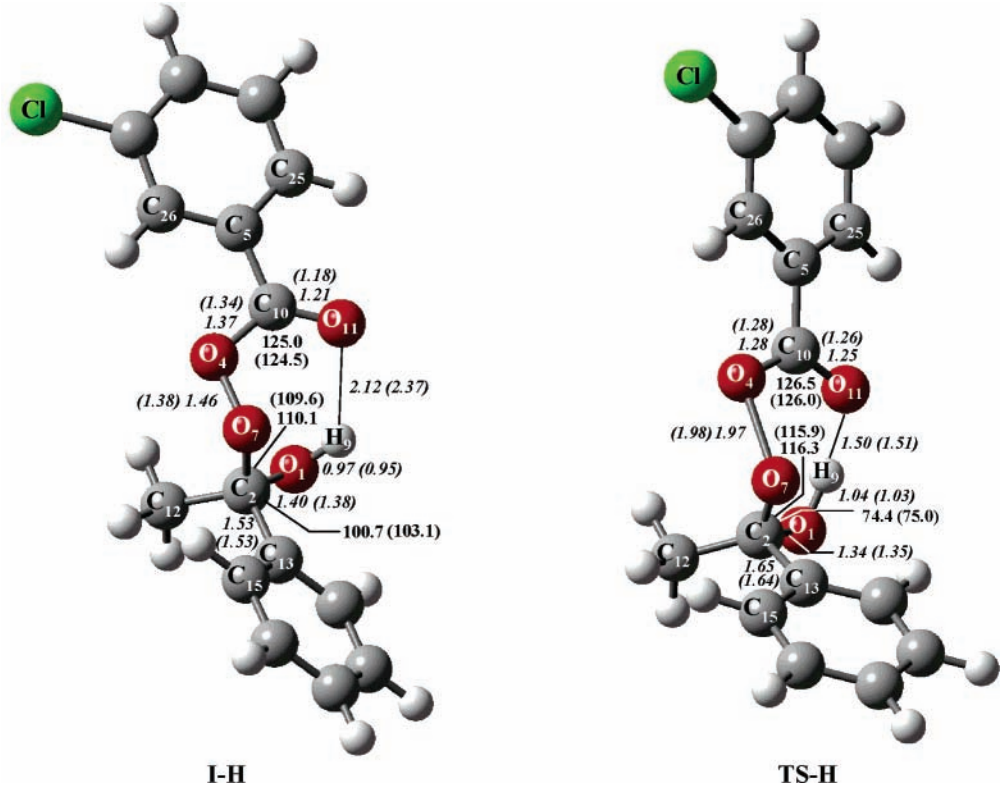

Figure 2. Optimized Criegee intermediate and transition structure for the BV rearrangement of acetophenone with *m*-CPBA at the B3LYP/6-31G** level. Bond lengths are in angstroms (italics) and bond angles in degrees. Values in parentheses correspond to the B3LYP/6-31+G** optimized structures.

TABLE 1: Selected Bond Lengths (Å) of Criegee Intermediates and Transition Structures for the BV Rearrangement of para-Substituted Acetophenones at the B3LYP/6-31G Level[a]**

structure	R	C_2-C_{13}	$C_{13}-O_7$	C_2-C_{12}	C_2-O_1	C_2-O_7	O_1-H_9	$O_{11}-H_9$	O_7-O_4	$C_{10}-O_4$	$C_{10}-O_{11}$	$C_{10}-C_5$	$C_{12}-O_7$
intermediate	CN	1.534	2.300	1.525	1.395	1.454	0.974	2.070	1.453	1.371	1.211	1.490	2.474
TS	CN	1.669	1.819	1.517	1.334	1.350	1.050	1.458	1.962	1.283	1.256	1.507	2.469
intermediate	Cl	1.532	2.299	1.525	1.396	1.454	0.974	2.092	1.455	1.369	1.211	1.491	2.473
TS	Cl	1.643	1.816	1.517	1.340	1.353	1.042	1.481	1.974	1.282	1.256	1.509	2.468
intermediate	H	1.532	2.301	1.525	1.396	1.455	0.973	2.118	1.455	1.368	1.211	1.492	2.473
		1.533	**2.303**	**1.525**	**1.399**	**1.457**	**0.973**	**2.168**	**1.456**	**1.370**	**1.212**	**1.493**	**2.476**
TS	H	1.649	1.829	1.518	1.342	1.350	1.037	1.498	1.966	1.283	1.255	1.509	2.466
		1.642	**1.838**	**1.518**	**1.348**	**1.353**	**1.033**	**1.514**	**1.967**	**1.285**	**1.256**	**1.510**	**2.473**
intermediate	CH_3	1.531	2.299	1.525	1.396	1.456	0.973	2.124	1.456	1.367	1.211	1.493	2.473
TS	CH_3	1.630	1.826	1.518	1.346	1.354	1.033	1.510	1.970	1.283	1.254	1.510	2.466
intermediate	CH_3O	1.529	2.296	1.525	1.397	1.456	0.973	2.113	1.458	1.367	1.211	1.493	2.473
TS	CH_3O	1.598	1.822	1.519	1.354	1.362	1.026	1.533	1.977	1.283	1.253	1.512	2.465

[a] Values in boldface type correspond to the B3LYP/6-31+G** optimized structures.

The Criegee intermediate plays an important role in the rate-determining step of the BV rearrangement. In previous work,[22] we observed that the structure of this intermediate involves the protonation of the carbonyl oxygen atom of the ketone, followed by the formation of the tetrahedral complex. From the point of view of the potential energy surface, this intermediate may be considered reactive in the rearrangement step. The optimized structures and the main geometrical parameters of the Criegee intermediates resulting from the reaction of *m*-CPBA with acetophenone, *p*-methylacetophenone, *p*-methoxyacetophenone, *p*-chloroacetophenone, and *p*-cyanoacetophenone, at the B3LYP/6-31G** level, are reported in Figure 2, Tables 1 and 2 (also see Figures 1S−4S in the Supporting Information). For the Criegee intermediate of the reference compound (acetophenone + *m*-CPBA, R = H; Figure 2), it can be observed that the distances between H_9 and O_1 (0.973 Å) and between H_9 and O_{11} (2.118 Å) suggest that the proton of H_9 starts to be ready to form a bond with the O_{11} atom in the transition state.

On the other hand, we have observed that, in the preferred conformation of the Criegee intermediate of the studied cases in this work, the aryl group (C_{13}) is closer to O_7 than the methyl moiety (C_{12}). As shown in Tables 1 and 2, the average values of the $C_{13}-O_7$ and $C_{12}-O_7$ bond lengths are 2.301 and 2.471 Å, respectively. This type of preference is also reflected by the smaller migration angle, $C_{13}-C_2-O_7$, associated with the aryl group, which is 100.7°. Meanwhile, the methyl group has a $C_{12}-C_2-O_7$ migration angle of 112.1°.

Moreover, the experimental evidence shows that the migrant group in the Criegee intermediate should be in an anti-periplanar position with respect to the outcoming oxygen atom, O_4.[35−40] Our results agree with this observation, considering that this intermediate displays $C_{13}-C_2-O_7-O_4$ dihedral angles between 177.1° and 177.5°, which are close to the expected angle, 180°.

The optimized transition structures of parent and substituted systems are presented in Figures 2 and 1S−4S and Tables 1−2. The C_2-C_{13}, C_2-O_1, $C_{13}-O_7$, O_7-O_4, and $O_{11}-H_9$ bond

TABLE 2: Dihedral Angles (°) of Criegee Intemediates and Transition Structures for the BV Rearrangement of para-Substituted Acetophenones at the B3LYP/6-31G Level[a]**

structure	R	$C_{10}-O_4-O_7-C_2$	$C_{13}-C_2-O_7-O_4$	$O_{11}-C_{10}-O_4-O_7$	$C_{15}-C_{13}-C_2-O_7$
intermediate	CN	99.5	177.1	12.8	49.5
TS	CN	81.4	176.6	25.6	86.8
intermediate	Cl	99.5	177.1	12.2	50.5
TS	Cl	81.5	177.3	25.5	86.5
intermediate	H	99.6	177.3	11.6	50.8
		101.0	**176.6**	**11.8**	**51.4**
TS	H	82.4	177.5	25.9	86.0
		81.1	**177.8**	**25.6**	**86.1**
intermediate	CH_3	99.5	177.5	11.4	51.3
TS	CH_3	82.0	177.7	25.4	86.1
intermediate	CH_3O	99.5	177.1	11.6	52.7
TS	CH_3O	81.6	178.9	25.2	85.9

[a] Values in boldface type correspond to the B3LYP/6-31+G** optimized structures.

lengths, the $C_{13}-C_2-O_7$ and $O_1-C_2-O_7$ bond angles, and the $C_{13}-C_2-O_7-O_4$ and $C_{15}-C_{13}-C_2-O_7$ dihedral angles are of particular interest and relevance, because they permit us to follow the structural changes in the migration step. In more detail, going from the intermediate adducts to the transition states, the C_2-C_{13} and O_7-O_4 bond lengths are increased by average values of 0.106 and 0.514 Å, respectively.

Contrarily, the bond lengths of C_2-O_1 and $C_{13}-O_7$ are shortened by average values of 0.053 and 0.477 Å, respectively, as the aryl group migrates toward the O_7 atom from the Criegee intermediates to the transition states. These findings suggest that both processes, the aryl transposition and the breaking of the peroxyl O_7-O_4 bond, are concerted.[22] Overall, the breaking of the C_2-C_{13} bond is much more susceptible to substitution than the formation of the $C_{13}-O_7$ bond; see Table 1. The calculated data show that the electron-withdrawing groups cause lengthening of the C_2-C_{13} bond with the exception of the *p*-Cl derivative, whereas the electron-donor groups induce a contrary effect, according to the observed ^{14}C isotope effect.[10]

On the other hand, the hydrogen bond between the H_9 and O_{11} atoms is shortened from an average of 2.103 to 1.496 Å, as the hydrogen migrates away from the O_1 atom in the intermediates to the transition states. These results suggest that this bond plays a stabilizing role in the TS.

The imaginary frequency values are in the 357.3−488.8i range (Tables 7S−11S in the Supporting Information). The animation of this clearly confirms that the migration step is a concerted process, because both C_2-C_{13} bond-breaking and $C_{13}-O_7$ bond-making are involved in the reaction vector that has a relatively small component of hydrogen migration.[29]

It should be noted that, with the exception of the *p*-CN derivative, the observed structural changes going from the Criegee adducts to the transition states make the dihedral angles $C_{13}-C_2-O_7-O_4$ even closer to being planar, as the dihedral angles are found to be in the 176.6−178.9° range. The average $C_{15}-C_{13}-C_2-O_7$ dihedral angle is 51.0° in the Criegee intermediates and 86.3° in the transition structures. Meanwhile, the $C_{13}-C_2-O_7$ migration angle decreases by an average of 23.3°, and the average bond angle $O_1-C_2-O_7$ is increased from 110.1° in the adducts to 116.2° in the transition states. These observations seem to adhere to the necessity of alignment of the molecular orbitals involved in the migration: the HOMO located on the aryl group with the LUMO on the acid moiety, as will be shown in the following text.

The calculated energies for the Criegee intermediate, TS, and products at several levels of theory for the parent and substituted cases are given in the Supporting Information, Table 1S. The energy barriers for the migration process, without ZPE corrections, range from 13.3 kcal/mol (X = OCH_3) to 19.4 kcal/mol (X = CN) at B3LYP/6-31G**. Using the MP2/6-31G** calculations at the B3LYP/6-31G** optimized geometries raises the B3LYP energy barrier by 6.9−8.5 kcal/mol. This result seems to be consistent with the indication that the B3LYP method underestimates the barriers for some reactions, as quoted already.[30] No experimental values are available for comparison.

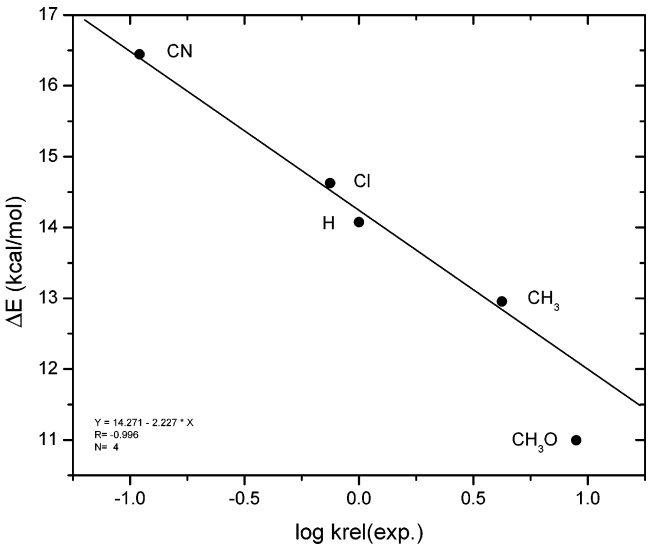

Figure 3. Plot of the log k_{rel} values for *m*-CPBA oxidation of the parent and para-substituted acetophenones vs their corresponding aryl migration barriers (relative to Criegee intermediate), ΔE, calculated using B3LYP/6-31G** total electronic energies with ZPE corrections.

Although the calculated energy barriers for the parent system change considerably at different levels of theory, there is a reasonable accord among the methods on the relative energy barriers for substituted cases. The data in Table 1S show that the magnitude of the energy barrier to migration varies with the electronic nature of the substituent group, and it is in the following order: CN > Cl > H > CH_3 > CH_3O. A plot of the log of relative rates of *m*-CPBA oxidation of the studied acetophenones[10] versus their calculated energy barriers, ΔE, of the aryl migration step at the B3LYP/6-31G** level reveals a quite good correlation, considering the neglect of solvent effects. This result seems to indicate that the rate-determining step for all these ketones is the migration of the aryl group. However, it was possible to obtain a better correlation by plotting the data without regard to the value for the *p*-methoxy group (see Figure 3). Although a small number of ketones was used, we can observe a clear downward deviation for the *p*-methoxy group. The MP2/6-31G**//HF/6-31G** and MP2/6-31G**//B3LYP/6-31G** energies reproduce a similar tendency. These findings are consistent with a change in the rate-determining step, from

TABLE 3: Orbital Energies for the HOMO and LUMO of the Criegee Intermediates and Relative Rates of *m*-CPBA Oxidation of para-Substituted Acetophenones

R	HOMO (eV)	LUMO (eV)	$\Delta E^a_{\mathrm{LUMO-HOMO}}$ (eV)	k (rel)[b]
CN	−9.582[c]	1.638	11.220	0.11
Cl	−9.155	1.764	10.919	0.75
H	−9.072	1.882	10.954	1.00
CH_3	−8.762	1.910	10.671	4.22
CH_3O	−8.428	1.911	10.340	8.90

[a] $\Delta E_{\mathrm{LUMO\ -\ HOMO}} = E_{\mathrm{LUMO}} - E_{\mathrm{HOMO}}$. [b] From ref 10. [c] The HOMO corresponds to the acid fragment, so the value is given for the next highest occupied molecular orbital (HOMO − 1) which is mainly located on the ester moiety.

the aryl migration to the carbonyl addition, in the case of *p*-methoxyacetophenone, according to Okuno's conclusion,[14] in which the rate-determining step of the BV oxidation can change with variations in the substituent group.

We can affirm that the reaction is exothermic observing the differences between the energies of the initial reactant (para-substituted acetophenone + *m*-chloroperbenzoic) and of the product (ester + *m*-chlorobenzoic acid). With B3LYP/6-31G**, these differences range from 64.1 kcal/mol (X = OCH_3) to 67.3 kcal/mol (X = CN) compared to 69.7−71.5 and 68.3−74.5 kcal/mol at the MP2/6-31G**//HF/6-31G** and MP2/6-31G**//B3LYP/6-31G**, respectively.

3.2. Natural Population Analysis. One further step in this study implies the understanding of electronic distribution change along the reaction path from the Criegee intermediate to the transition state. For this purpose, we performed an NPA and separated the structures into two fragments: the acid and the ester moieties. The charge distribution on the Criegee adduct and the TS for the compounds under investigation are presented in Figure 4. In all of them, a partial negative charge is on the acid fragment and a partial positive charge is on the ester part. In the transition state of the parent compound, the charge separation is 0.44 e. The transition state of the substituted cases shows little change in polar character with respect to that of the reference compound. The resultant dipole moment at the TS varies from 2.22 to 8.14 D.

As can be anticipated, electron-donor groups, CH_3 and OCH_3, at C_{14} can stabilize the partial positive charge present at the ester part of the TS structure. In contrast, the electron-withdrawing groups, Cl and CN, at the same position, are not expected to stabilize the ester moiety. We found a relationship between the energy barriers at the B3LYP/6-31G** level for the migration process and the Hammett electronic parameter[41] σ^+ in the form of $\Delta E = 14.07 + 3.80\sigma^+$ ($n = 5$, $r = 0.998$). This result implies an invariant pattern for the TS structures. That is, the reaction mechanism would be the same for all the studied cases. However, the downward deviation observed[11] for the *p*-OCH_3 substituent in the Hammett correlations with σ^+ suggests a change of mechanism for this case, as discussed already.

3.3. Frontier Molecular Orbitals Analysis. It is possible to explain the migration step like an electron transfer from the HOMO of the migrating aryl group to the LUMO of the O_7-O_4 bond. Thus, the way that substituents influence the reactivity of the studied ketones can be analyzed by considering how they interact with the frontier molecular orbitals of the Criegee intermediate.[42,43] An analysis of these molecular orbitals reveals that, for this adduct, the HOMOs are associated principally with the π system of the migrating aryl group. For instance, the spatial distribution of this orbital is slightly more concentrated around C_{13}. For the CN derivative, the HOMO corresponds to the acid fragment; so, in this case, HOMO − 1 is located on the ester fragment. Meanwhile, the LUMO is associated with the acid moiety of all the intermediates. It is worthy to mention that this orbital does not lie at the O_7 atom (Figure 5), as expected from the negative charge present on this atom. Substitution on the Criegee adduct changes the HOMO energies significantly and the LUMO ones slightly (see Table 3). Both orbitals are destabilized by electron-donor groups, whereas the electron-withdrawing groups interact with them in a stabilizing way. This leads to a decrease of the $\Delta E_{\mathrm{HOMO-LUMO}}$ gaps, according to the observed reactivities, with the exception of the chloro compound.[44] However, it was possible to determine a good correlation between the HOMO energies of the Criegee adducts with the energy barrier of the migration in the form of $\Delta E = -28.06 - 4.65E_{\mathrm{HOMO}}$ ($n = 5$, $r = 0.997$). This correlation is best explained by involving, in the TS, an interaction between the HOMO of the aryl group and the LUMO on the acid moiety.

The Criegee intermediates, which possess higher HOMO energy levels, correspond to acetophenones with higher relative reactivity. As expected, an excellent relationship was obtained by plotting these HOMO energies versus the log of the experimental relative reaction rates for the ketones under study without considering the value of the *p*-methoxyacetophenone (Figure 6).

3.4. Evolution of the Bond Orders. The progress of the migration process can also be studied by observing the differences in bond orders. Theoretically, if the differences at the TS are close to zero, we can consider that the atom binds the donor and the acceptor with roughly the same bond order. If the differences are negative, it means that it is more associated with the donor than the acceptor.

Correspondingly, if they are positive, the opposite is true. Table 3 shows that, at the TS of the parent system, while the O_7 atom binds to C_{13} and O_4 with nearly the same order (0.04), the aryl group (C_{13}) is more associated with its donor C_2, than the receptor O_7 (−0.31). These results would imply a concerted and asynchronous transposition, in which the O_7-O_4 bond-breaking process is more advanced than the aryl migration. This description reveals the TS in an early stage of the migration path closer to the Criegee intermediate than to the products, in agreement with the Hammond postulate[45] considering the obtained energy barrier.

It is important to note that the synchronicity can vary with respect to the chosen computational method and model system, as we have demonstrated in our previous study.[22] In this case, the DFT calculations describe the TS in a slightly more

TABLE 4: Changes in Bond Orders for Aryl Migration, Oxygen Break, and Hydrogen Transfer

	Ar $n(C_{13}-O_7)-n(C_2-C_{13})$			O $n(C_{13}-O_7)-n(O_7-O_4)$			H $n(H_9-O_{11})-n(H_9-O_1)$		
R	adduct	TS	P	adduct	TS	P	adduct	TS	P
CN	−0.95	−0.27	0.82	−0.88	0.05	0.84	−0.76	−0.38	0.85
Cl	−0.95	−0.30	0.80	−0.88	0.06	0.82	−0.76	−0.41	0.85
H	−0.95	−0.31	0.79	−0.88	0.04	0.81	−0.77	−0.42	0.85
CH3	−0.95	−0.33	0.79	−0.87	0.05	0.80	−0.77	−0.44	0.85
OCH3	−0.95	−0.38	0.78	−0.87	0.06	0.80	−0.77	−0.46	0.85

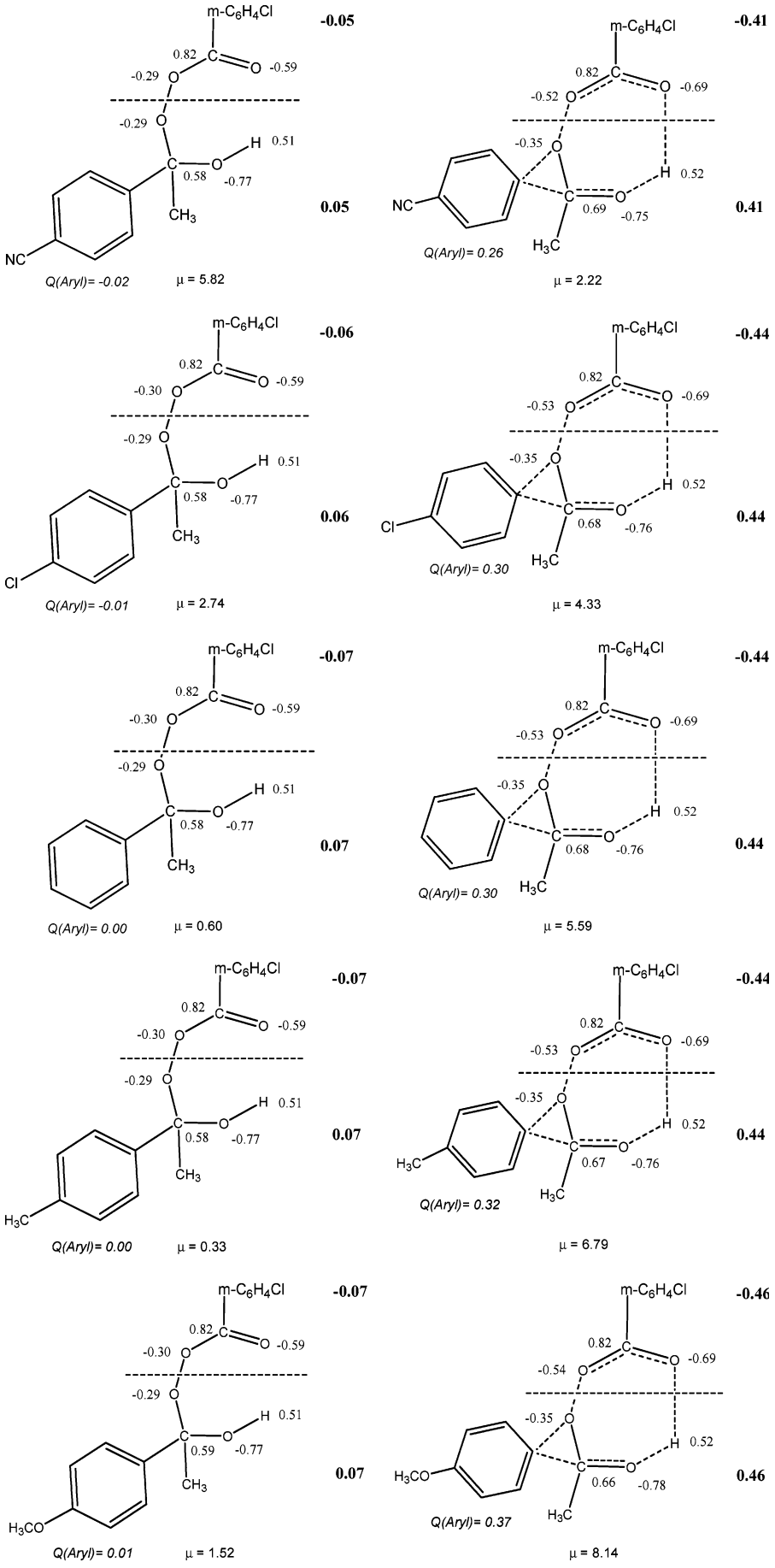

Figure 4. Charge distribution of NPA analysis in the Criegee intermediates and TSs of parent and para-substituted acetophenones at the B3LYP/6-31G** level. The dashed line separates the acid moiety from the ester fragment; their charges are shown in boldface type.

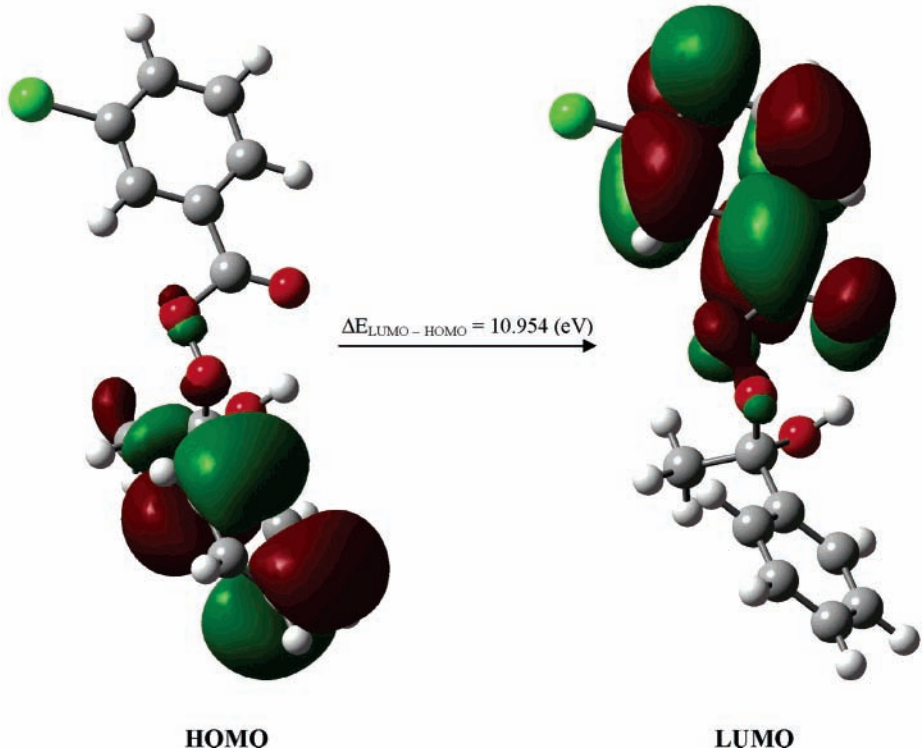

Figure 5. HOMO and LUMO contour plots for the Criegee intermediate of the oxidation of acetophenone with *m*-CPBA.

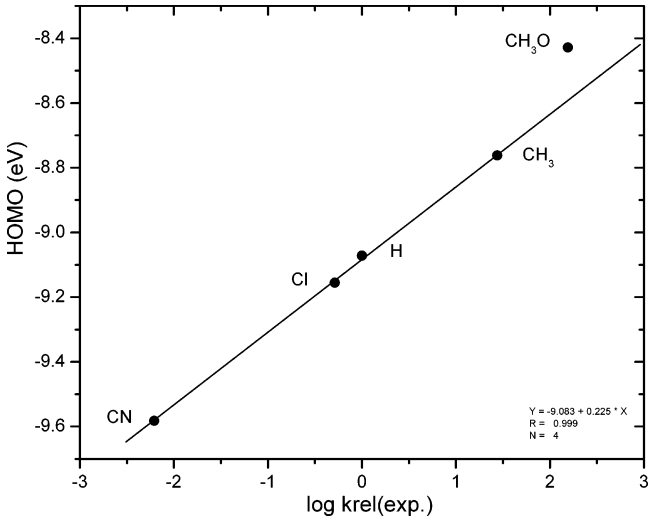

Figure 6. Plot of the log k_{rel} values for *m*-CPBA oxidation of the parent and para-substituted acetophenones vs the HOMO energies of their corresponding Criegee intermediates.

advanced stage for the aryl transfer than the Hartree−Fock method. From the aryl migration data, in Table 4, it is possible to find that the electron-donor groups, CH_3 and OCH_3, induce the formation of an earlier TS than for the parent system, while the electron-withdrawing groups cause a contrary effect. This tendency is consistent with experimental results.[10]

Finally, considering the proton-transfer process, we can observe for all the acetophenones that while the proton of H_9 is still tightly united to its donor O_1, at the TS, the aryl group has already advanced toward the O_7.

4. Conclusions

The mechanism for the BV rearrangement of para-substituted acetophenones $CH_3COC_6H_4$−R (R = CN, Cl, H, CH_3, CH_3O) with *m*-chloroperbenzoic acid has been theoretically studied. The calculations focus at the aryl group migration step and are based on the geometric optimization at the B3LYP/6-31G** level, including the electron correlation effect at the MP2 procedure: MP2/6-31G**//HF/6-31G** and MP2/6-31G**//B3LYP/6-31G**. Although specific details of the migration process may change by solvent effects and/or higher levels of theory, some important aspects were elucidated.

An analysis of bond order shows that the process corresponds to a concerted and asynchronous transposition. The O_7−O_4 bond-breaking process is more advanced than the aryl migration. A charge separation in the TS for the rearrangement of para-substituted acetophenones shows its weak dipolar character.

Energy barriers, charge distributions, frontier molecular orbitals, and bond order analysis of the TS account for the effects of substituents on the rates of BV rearrangement. A plot of the relative oxidation rates of these ketones versus their corresponding calculated energy barriers of the migration stage at the B3LYP/6-31G** shows a deviation for the *p*-OCH_3 derivative. This result is consistent with a change in the rate-determining step, from the aryl migration to the carbonyl addition, in the case of *p*-methoxyacetophenone, according to Okuno's suggestion, in which the rate-determining step of the BV oxidation can change with variations in the substituent group.

Acknowledgment. M.C. acknowledges financial support from DGAPA-UNAM under project PAPIIT-IN-101901. The authors thank Dr. I. Nicolás for her valuable discussions. The access to the supercomputer Silicon Graphics Origin 2000/32 at DGSCA-UNAM is strongly appreciated.

Supporting Information Available: Total energies and Cartesian coordinates of the Criegee intermediates and TSs for the BV rearrangement of parent and para-substituted acetophenones with *m*-CPBA at the B3LYP/6-31G** level of theory are shown in Tables 1S−11S. The Cartesian coordinates of optimized structures at the B3LYP/6-31+G** level are presented in Tables 12S and 13S. Figures 1S−4S contain additional

optimized structures obtained at the B3LYP/6-31G** level of theory. This material is available free of charge via the Internet at http://pubs.acs.org.

References and Notes

(1) Baeyer, A.; Villiger, V. *Ber. Dtsch. Chem. Ges.* **1899**, *32*, 3625.
(2) Krow, G. R. *Org. React.* **1993**, *43*, 251.
(3) Renz, M.; Meunier, B. *Eur. J. Org. Chem.* **1999**, 737.
(4) ten Brink, G.-J.; Arends, I. W. C. E.; Sheldon, R. A. *Chem. Rev.* **2004**, *104*, 4105.
(5) Criegee, R. *Justus Liebigs Ann. Chem.* **1948**, *560*, 127.
(6) Doering, W. E.; Dorfman, E. *J. Am. Chem. Soc.* **1953**, *75*, 5595.
(7) Friess, S. L.; Soloway, A. H. *J. Am. Chem. Soc.* **1951**, *73*, 3968.
(8) Hawthorne, M. F.; Emmonds, W. D. *J. Am. Chem. Soc.* **1958**, *80*, 6398.
(9) Mitsuhashi, T.; Miyadera, H.; Simamura, O. *J. Chem. Soc., Chem. Commun.* **1970**, 1301.
(10) Palmer, B. W.; Fry, A. *J. Am. Chem. Soc.* **1970**, *92*, 2580.
(11) Ogata, Y.; Sawaki, Y. *J. Org. Chem.* **1972**, *37*, 4189.
(12) Ogata, Y.; Sawaki, Y. *J. Am. Chem. Soc.* **1972**, *94*, 4189.
(13) Snowden, M.; Bermúdez, A.; Kelly, D. R.; Radkiewicz-Poutsma, J. L. *J. Org. Chem.* **2004**, *69*, 7148.
(14) Itoh, Y.; Yamakata, M.; Mikami, K. *Org. Lett.* **2003**, *5*, 4803.
(15) Okuno, Y. *Chem.—Eur. J.* **1997**, *3*, 212.
(16) Kobayashi, S.; Tanaka, H.; Amii, H.; Uneyama, K. *Tetrahedron* **2003**, *59*, 1547.
(17) Kitazume, T.; Kataoka, J. *J. Fluorine Chem.* **1996**, *80*, 157.
(18) Stoute, V. A.; Winnik, M. A.; Csizmadia, I. G. *J. Am. Chem. Soc.* **1974**, *96*, 6388.
(19) Rubio, M.; Cetina, R.; Bejarano, A. *Afinidad* **1983**, *40*, 176.
(20) Rubio, M.; Reyes, L.; Cetina, R.; Pozas, R. *Afinidad* **1989**, *46*, 341.
(21) Hannachi, H.; Anoune, N.; Arnaud, C.; Lantéri, P.; Longeray, R.; Chermette, H. *THEOCHEM* **1998**, *434*, 183.
(22) Cárdenas, R.; Cetina, R.; Lagunez-Otero, J.; Reyes, L. *J. Phys. Chem.* **1997**, *101*, 192.
(23) Cárdenas, R.; Reyes, L.; Lagunez-Otero, J.; Cetina, R. *THEOCHEM* **2000**, *497*, 211.
(24) Lehtinen, C.; Nevalainen, V.; Brunow, G. *Tetrahedron Lett.* **2000**, *56*, 9375.
(25) Carlqvist, P.; Eklund, R.; Brinck, T. *J. Org. Chem.* **2001**, *66*, 1193.
(26) Sever, R. R.; Root, T. W. *J. Phys. Chem. B* **2003**, *107*, 10848.
(27) Frisch, M. J.; Trucks, G. W.; Schlegel, H. B.; Scuseria, G. E.; Robb, M. A.; Cheeseman, J. R.; Zakrzewski, V. G.; Montgomery, J. A., Jr.; Stratmann, R. E.; Burant, J. C.; Dapprich, S.; Millam, J. M.; Daniels, A. D.; Kudin, K. N.; Strain, M. C.; Farkas, O.; Tomasi, J.; Barone, V.; Cossi, M.; Cammi, R.; Mennucci, B.; Pomelli, C.; Adamo, C.; Clifford, S.; Ochterski, J.; Petersson, G. A.; Ayala, P. Y.; Cui, Q.; Morokuma, K.; Malick, D. K.; Rabuck, A. D.; Raghavachari, K.; Foresman, J. B.; Cioslowski, J.; Ortiz, J. V.; Stefanov, B. B.; Liu, G.; Liashenko, A.; Piskorz, P.; Komaromi, I.; Gomperts, R.; Martin, R. L.; Fox, D. J.; Keith, T.; Al-Laham, M. A.; Peng, C. Y.; Nanayakkara, A.; Gonzalez, C.; Challacombe, M.; Gill, P. M. W.; Johnson, B. G.; Chen, W.; Wong, M. W.; Andres, J. L.; Head-Gordon, M.; Replogle, E. S.; Pople, J. A. *Gaussian 98*, revision A.7; Gaussian, Inc.: Pittsburgh, PA, 1998.
(28) *SPARTAN*, version O2; Wavefunction, Inc.: 18401 Von Karman Ave., Suite 370, Irvine, CA 92612, U.S.A.
(29) Bach, R. D.; Dmitrenko, O. *J. Phys. Chem. B* **2003**, *107*, 12851.
(30) Zhang, Q.; Bell, R.; Truong, T. N. *J. Phys. Chem.* **1995**, *99*, 592.
(31) Durant, J. L. *Chem. Phys. Lett.* **1996**, *256*, 595.
(32) Hu, C.; Brinck, T. *J. Phys. Chem. A* **1999**, *103*, 5379.
(33) Reed, A. E.; Curtiss, L. A.; Weinhold, F. *Chem. Rev.* **1988**, *88*, 899.
(34) Mayer, I. *Int. J. Quantum Chem.* **1986**, *29*, 477.
(35) Noyori, R.; Kobayashi, H.; Sato, T. *Tetrahedron Lett.* **1980**, *21*, 2573.
(36) Noyori, R.; Sato, T.; Kobayashi, H. *Tetrahedron Lett.* **1980**, *21*, 2569.
(37) Chandrasekhar, S.; Roy, C. D. *Tetrahedron Lett.* **1987**, *28*, 6371.
(38) Chandrasekhar, S.; Roy, C. D. *J. Chem. Soc., Perkin Trans. 2* **1994**, 2141.
(39) Goodman, R. M.; Kishi, Y. *J. Am. Chem. Soc.* **1998**, *120*, 9392.
(40) Crudden, C. M.; Chen, A. C.; Calhound, L. A. *Angew. Chem., Int. Ed.* **2000**, *39*, 2851.
(41) Hansh, C.; Leo, A.; Taft, R. W. *Chem. Rev.* **1991**, *91*, 165.
(42) Fleming, I. *Frontier Orbitals and Organic Chemical Reactions*; John Wiley and Sons: New York, 1976.
(43) Henri-Rousseau, O.; Texier, F. *J. Chem. Educ.* **1978**, *55*, 437.
(44) Puzzarini, C.; Cazzoli, G. *J. Phys. Chem.* **2003**, *118*, 2647.
(45) Hammond, G. S. *J. Am. Chem. Soc.* **1955**, *77*, 334.